Biophysical Journal, Volume *120*

Supplemental Information

Fat inclusions strongly alter membrane mechanics

Alexandre Santinho, Aymeric Chorlay, Lionel Foret, and Abdou Rachid Thiam

Supplemental figures

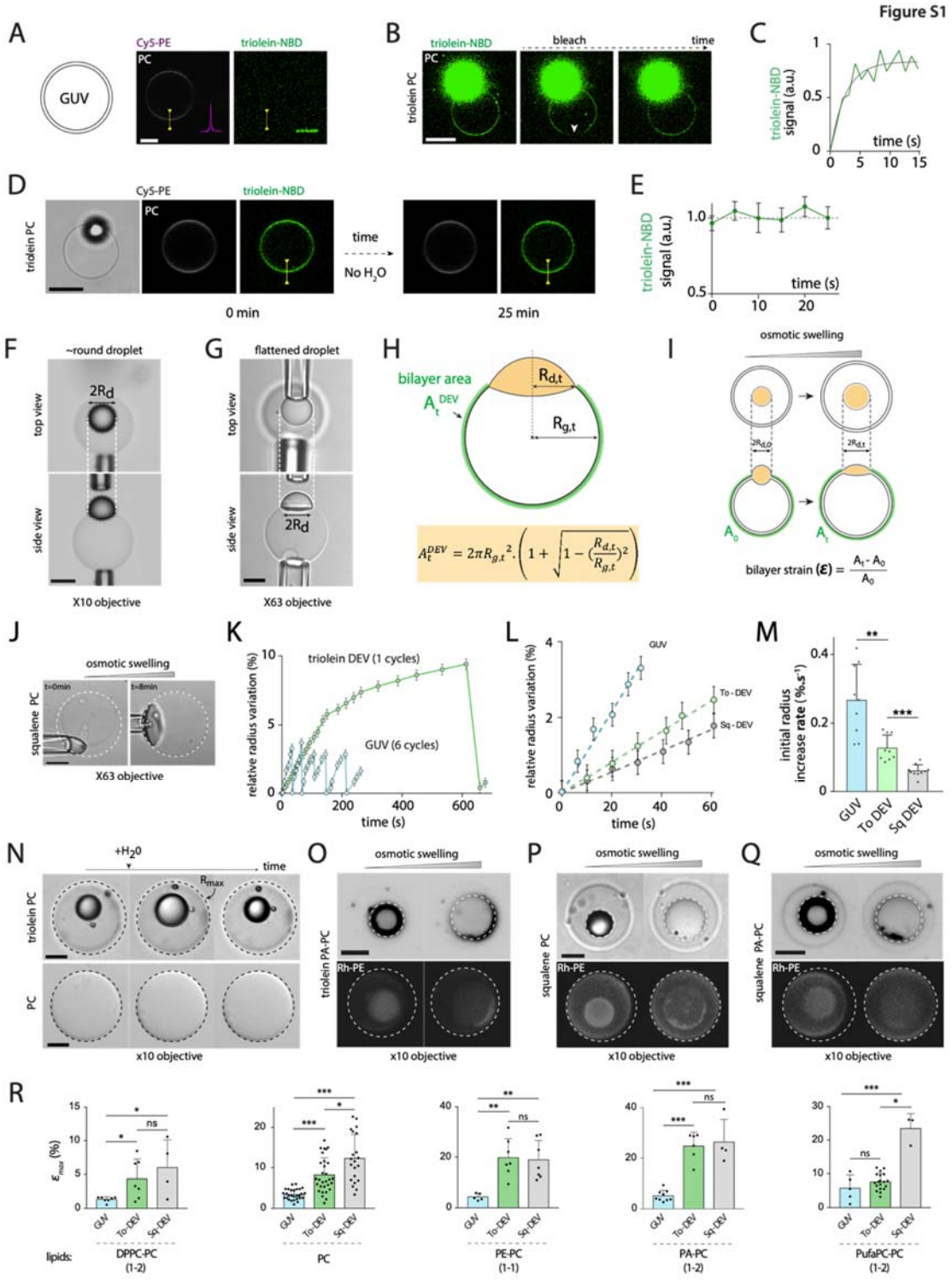

Figure S1: related to figure 1

A) Confocal images of a PC GUV marked with Cy5-PE. The same settings as in Figure 2B were used for the green channel. No signal of triolein-NBD was visible here. Scale bar: 5µm. **B)** Confocal images of PC DEVs of triolein supplemented with 0,05% (w/w) triolein-NBD to report for triolein distribution. Image sequence of a FRAP (Fluorescence Recovery After Photobleaching) experiment on the bilayer. After bleaching the bilayer (see arrowhead), the triolein-NBD signal recovered. The scale bar is 5µm. **C)** Over time quantification of normalized triolein-NBD fluorescence signal after bleaching showing recovery. The non-linear fit matches the FRAP recovery curve. The fit was done with an exponential "one-phase association model". **D)** Confocal images of PC DEVs of triolein supplemented with triolein-NBD. The triolein DEVs were imaged for 25 minutes with no osmotic shock. The scale bar is 10µm. **E)** Over time variations of the triolein NBD-signal in the bilayer shows no variation of triolein concentration during 25 minutes. Absolute value +/- measurement uncertainty. **F)** Confocal bright field images captured at x10 objective of single PC DEV of triolein at a low tension state. Top view and side view showing the same droplet radius (R_d) used to compute the initial bilayer area of a DEV. The scale bar is 10µm. **G)** Confocal bright field images captured at x63 objective of single PC DEV of triolein at a high tension state with a flattened droplet. Top view and side view showing the same droplet radius (R_d) used to compute the final bilayer area of a DEV. The scale bar is 5µm. **H) Top:** Illustration of a DEV and needed parameters to compute the DEV bilayer area subtracting the area occupied by the embedded droplet. **Bottom:** Equation used to compute the bilayer area of a DEV. **I) Top:** Schematic representation of the bilayer area variations during osmotic swelling of a DEV (top view and side view). Green arcs underly the bilayer area. **Bottom:** Equation used to compute the bilayer strain ε. **J)** Representative images of a PC squalene-DEV observed at x63 objective during a hypotonic shock experiment. The first image corresponds to the unswollen state and the second to one of the critical bilayer strain before burst. Dashed circles report maximum radius. Scale bar: 10µm. **K)** Related to Figure 1B. The plot of the relative vesicle radius variations of triolein DEV and GUV over time. Swelling and burst cycles are visible for GUVs (blue points; 6 cycles) and DEVs (green points; 1 cycle). Absolute value +/- measurement uncertainty. **L)** Plot of the vesicle relative radius variation at the beginning of a swelling experiment of a GUV (blue points), a triolein DEV (green points), and a squalene DEV (grey points). The slope of the linear fit (dotted lines on the graph) was used to determine the initial radius increase rate. Absolute value +/- measurement uncertainty. **M)** Plot of the initial radius increase rate of PC bilayer of GUVs (n=8), triolein-DEVs (n=9), and squalene DEVs (n=9). Mean +/- SD. **N)** Time-lapse of triolein DEV and GUV during a

hypotonic shock experiment. Black dashed circles report maximum radius. The scale bar is 5µm. **O)** Representative images of a PC-PA triolein-DEV during a hypotonic shock experiment. The first image corresponds to the unswollen state and the second to the bilayer critical strain before burst. Dashed circles report maximum radius. Scale bar: 10µm. **P)** Representative images of a PC squalene-DEV during a hypotonic shock experiment. The first image corresponds to the unswollen state and the second to the bilayer critical strain before burst. Dashed circles report maximum radius. Scale bar: 10µm. **Q)** Representative images of a PC-PA squalene-DEV during a hypotonic shock experiment. The first image corresponds to the unswollen state and the second to the bilayer critical strain before burst. Dashed circles report maximum radius. Scale bar: 10µm. **R)** Detailed plots of figure 1F. Critical bilayer strain is shown for each phospholipids conditions with a student t-test. Stars indicate if means are significantly different or not. Mean +/- SD.

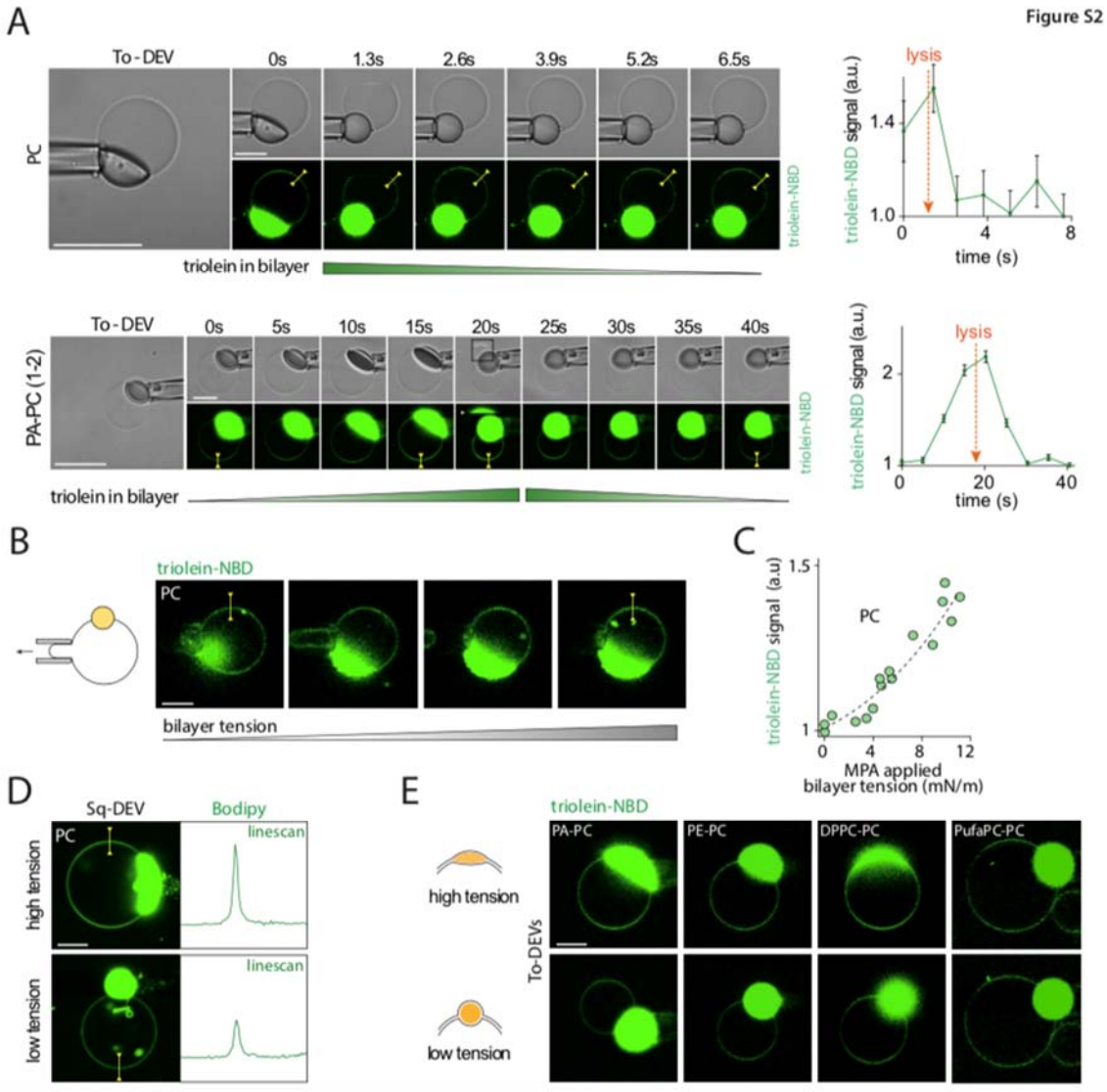

Figure S2: related to figure 2

A) Top: Time course of confocal images of a PC triolein-DEV (left) just after the burst of the vesicle. The scale bar is 20µm. Corresponding quantification of the amount of oil (right) in the bilayer shows a fast recovery of low triolein level after burst (few seconds). Absolute value +/- measurement uncertainty. **Bottom**: Time coarse of confocal images of a PC-PA triolein-DEV (left) before and after the burst. The scale bar is 20µm. Corresponding quantification of the amount of oil (right) in the bilayer shows a fast increase of oil level before burst followed by a rapid decrease of oil level after burst (few seconds). Absolute value +/- measurement uncertainty.

B) Left, Illustration of the method used to increase the bilayer tension of a triolein-DEV thanks to the micropipette aspiration technique. **Right**, the triolein-NBD signal in the bilayer of a PC triolein-DEVs during MPA-applied bilayer tension increase. Scale bar: 5µm. **C)** Plot of the triolein-NBD signal in bilayer against MPA-applied bilayer tension for PC triolein-DEVs. n=4 experiments. **D)** Confocal images of PC Sq-DEVs during the swelling experiment with bodipy, a hydrophobic probe. Scale bar: 5µm. A line scan of the bodipy signal in the bilayer is shown both in the stretched and unstretched state. **E)** Visualization of triolein-NBD signal in the bilayer during a hypotonic shock of PA-PC, PE-PC, DPPC-PC, and PufaPC-PC of triolein-DEVs both in the stretched and unstretched state. Scale bar: 5µm.

Figure S3

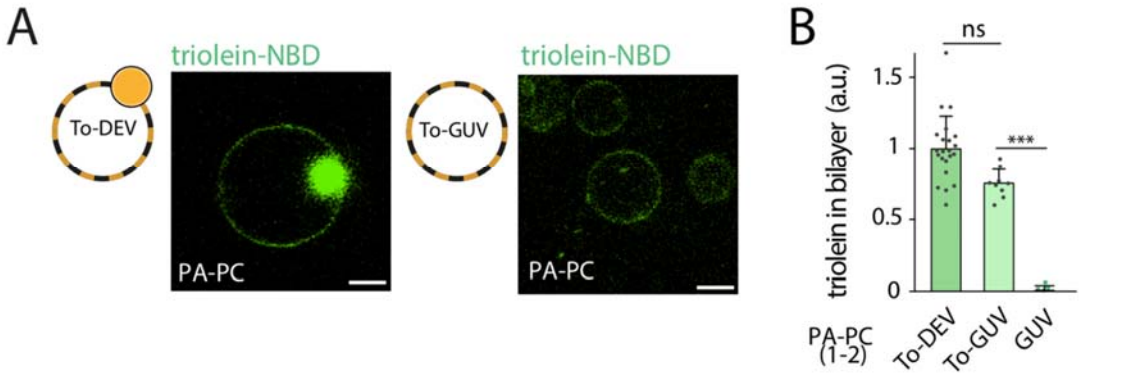
A
triolein-NBD
To-DEV
PA-PC
triolein-NBD
To-GUV
PA-PC
B
ns
***
triolein in bilayer (a.u.)
1.5
1
0.5
0
PA-PC (1-2)
To-DEV
To-GUV
GUV

Figure S3: related to figure 3

A) Confocal images of PA-PC triolein-DEV and triolein-GUV with triolein-NBD. Scale bar: 5µm. **B)** Plot of the triolein in bilayer for PC-PA GUVs (n=4), triolein-GUVs (n=9), and triolein-DEVs (n=22). Mean +/- SD.

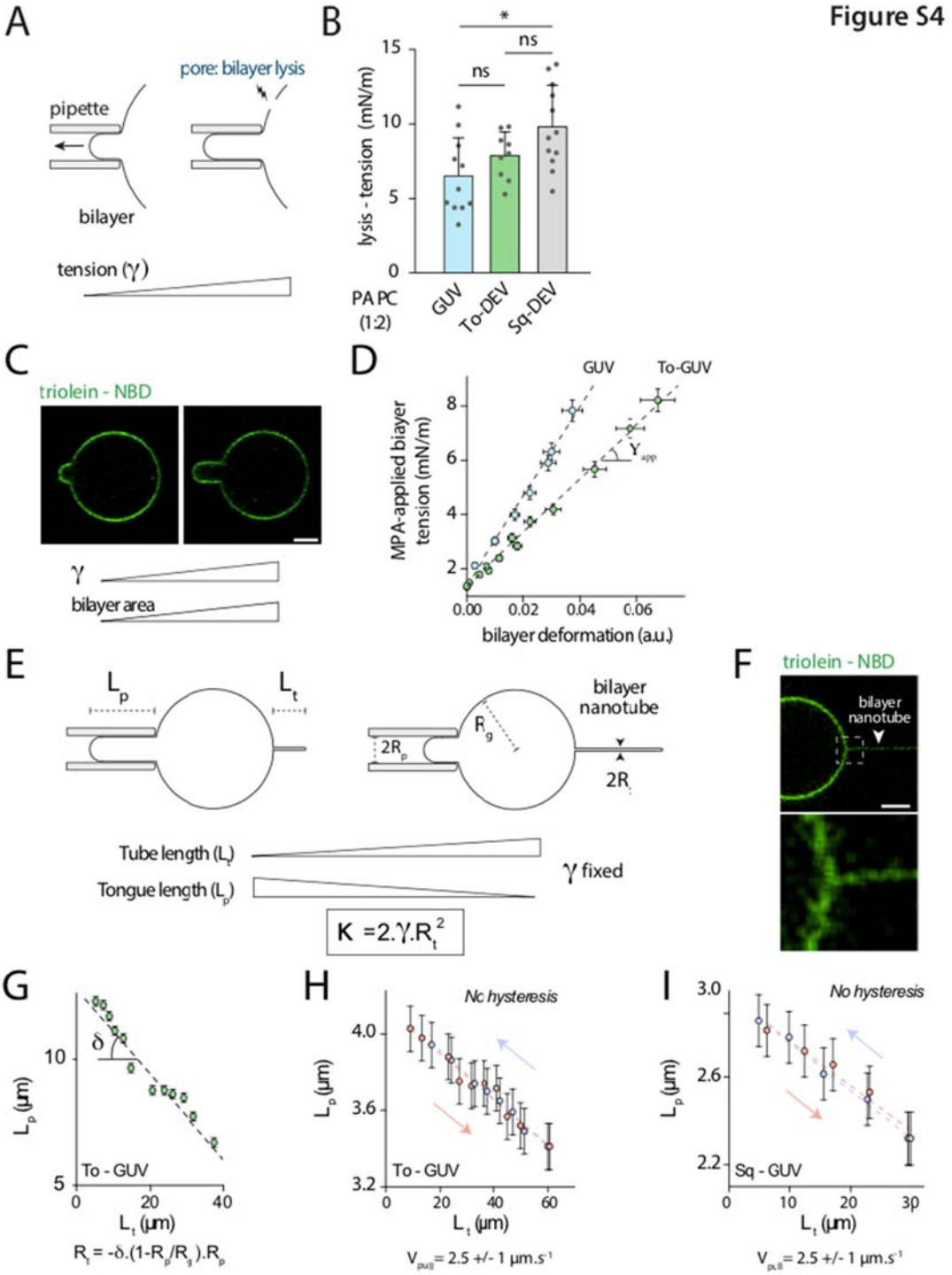
Figure S4
A
pore: bilayer lysis
pipette
bilayer
tension (γ)
B
*
ns
ns
lysis - tension (mN/m)
15
10
5
0
PA PC (1:2)
GUV
To-DEV
Sq-DEV
C
triolein - NBD
γ
bilayer area
D
GUV
To-GUV
MPA-applied biayer tension (mN/m)
8
6
4
2
0.00
0.02
0.04
0.06
bilayer deformation (a.u.)
E
L_p
L_t
2R_p
R_g
bilayer nanotube
2R_t
Tube length (L_t)
Tongue length (L_p)
γ fixed
K =2.γ.R_t^2
F
triolein - NBD
bilayer nanotube
G
δ
10
5
L_p (μm)
To - GUV
0
20
40
L_t (μm)
R_t = -δ.(1-R_p/R_g).R_p
H
Nc hysteresis
4.0
3.6
3.2
L_p (μm)
To - GUV
0
20
40
60
L_t (μm)
V_pull= 2.5 +/- 1 μm.s^-1
I
No hysteresis
3.0
2.6
2.2
L_p (μm)
Sq - GUV
0
10
20
30
L_t (μm)
V_p,II= 2.5 +/- 1 μm.s^-1

Figure S4: related to figure 4

A) Illustration of the method used for lysis tension determination. The bilayer tension of a vesicle is raised with a micropipette until the bilayer ruptures. Lysis tension is taken as the higher sustainable tension just before rupture. **B)** Membrane lysis tension of GUVs (n=11), triolein-DEVs (n=9) and squalene-DEVs (n=12) made with PC-PA. Mean +/- SD. **C)** Confocal images corresponding to the determination of the apparent area expansion modulus on a triolein-GUV with a triolein-NBD signal. Membrane tension is raised and the associated variation of the area is recorded. Scale bar: 5µm. **D)** Plot of the MPA-applied bilayer tension against area relative variation for a PC GUV (blue points) and a PC triolein-GUV (green points). Absolute value +/- measurement uncertainty. The slopes of the linear fits (dotted lines) are the elastic modulus of the corresponding GUV and triolein-GUV. **E)** Illustration of the determination protocol of the bending modulus computed with the membrane tension and the tube radius obtained by varying the tube length and recording the associated tongue length. **F)** Confocal images of a nanotube pulled from a PC triolein-DEV. Scale bar: 5µm. Zoom on the nanotube where a triolein-NBD signal is visible. Scale bar: 1µm. **G)** Example of a tongue length against tube length plot. The slope is linked with the nanotube radius which then allows computing the bending modulus. **H)** Tongue length against tube length plot for a triolein-GUV. The nanotube is pulled (red points) from the triolein-GUV and pushed (blue points) towards the triolein-GUV at a constant velocity of 2.5 +/- 1µm/s. Absolute value +/- measurement uncertainty. No hysteresis was detected indicating that oil partitioning is at the equilibrium during the tube pulling experiment. **G)** Tongue length against tube length plot for a squalene-GUV. The nanotube is pulled (red points) from the squalene-GUV and pushed (blue points) towards the squalene-GUV at a constant velocity of 2.5 +/- 1µm/s. Absolute value +/- measurement uncertainty. No hysteresis was detected indicating that oil partitioning is at equilibrium during the experiment.

Supplemental Text.

Supplementary materials: initial permeability determination for GUVs and DEVs

A. Fick law: conditions of utilization

Diffusion times of solutes through a phospholipid bilayer are negligible compared to the diffusion time of water. We therefore considered the diffusion of solutes through the bilayer of GUVs (or DEVs) as negligible compared to the diffusion of water. In this condition, Fick law leads to:

$$\frac{dV_t}{dt} = -\boldsymbol{P}.S_t.v_m.\Delta C(t)$$

where V_t is the volume inside the vesicle delimitated by S_t the area of permeation (ie area of bilayer), P the bilayer permeability to water, v_m the molar volume of water (18g.mol^{-1}) and $\Delta C(t)$ the difference of solutes concentration between the outside $C^e(t)$ and the inside $C^i(t)$ of the vesicle.

$$\Delta C(t) = C^e(t) - C^i(t)$$

B. $\Delta C(t)$: hypothesis and computation as a function of $R_{g,t}$

In our experiments, we considered only the first cycle of swelling and the first minute of experiment because it is difficult to characterize the concentration of solutes inside a GUV or a DEV after the first burst. We assume the concentration of solutes in the buffer to be constant and equal to the initial outside concentration C_0^e (145mOsm) as the buffer volume (220µL) is far greater than the volume of the vesicles having a radius between 5µm and 15µm (between 1pL and 15pL in volume). The concentration in the vesicle is equal to the initial one adjusted by the dilution factor $\frac{V_0}{V_t}$ where V_0 is the initial volume of the vesicle.

$$\Delta C(t) = C_0^e - C_0^i.\frac{V_0}{V_t} = C_0^i.(\frac{C_0^e}{C_0^i} - \frac{R_{g,0}^3}{R_{g,t}^3})$$

Where $R_{g,t}$ and $R_{g,0}$ are respectively the vesicle radius at the time t and at the beginning of swelling (**Figure 1**). As we have small variations of radius (<10%). We made the approximation that:

$$R_{g,t} = \delta R_{g,t} + R_{g,0}$$

where $\delta R_{g,t}$ represent the small variations of vesicle radius.

It follows that:

$$\Delta C(t) = C_0^i.\left(\frac{C_0^e}{C_0^i} - \frac{1}{(1+\frac{\delta R_{g,t}}{R_{g,0}})^3}\right)$$

At the first order we have:

$$\Delta C(t) = C_0^i.\left(\frac{C_0^e}{C_0^i} + \left(3\frac{\delta R_{g,t}}{R_{g,0}} - 1\right)\right)$$

Then we have:

$$\Delta C(t) = C_0^i.\left(\frac{C_0^e}{C_0^i} + 3\frac{R_{g,t}}{R_{g,0}} - 4\right)$$

Now that $\Delta C(t)$ is determine, in next, C&D, we will determine the exact surface and volume of DEV involve in the Fick law.

C. GUV and DEV permeation surface: hypothesis and computation as a function of $R_{g,t}$

The permeation surface of the GUV (S_t^{GUV}) corresponds to the surface of the sphere formed by its bilayer and can be expressed as:

$$S_t^{GUV} = 4\pi {R_{g,t}}^2$$

In the case of the DEV, the water cannot pass through the oil droplet. Thus to assess the permeation surface of a DEV (S_t^{DEV}) we have to subtract the surface area occupied by the droplet S_t^{cap} from the surface area of the sphere forming its bilayer S_t^{GUV} (see **Figure 1**) :

$$S_t^{DEV} = S_t^{GUV} - S_t^{cap}$$

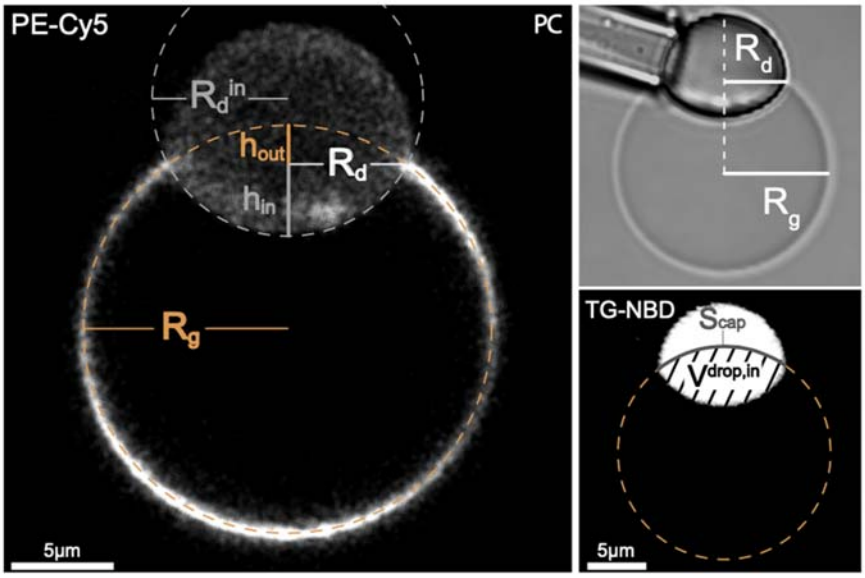

Figure 1: triolein-DEVs of DOPC at x63 objective showing parameters to compute the corrected surface and volume of a DEV.

Note that both S_t^{cap} and S_t^{GUV} (**Figure 1**) are varying over time due to the variations of the vesicle $R_{g,t}$ and the droplet radii $R_{d,t}$ (**Figure 2**).

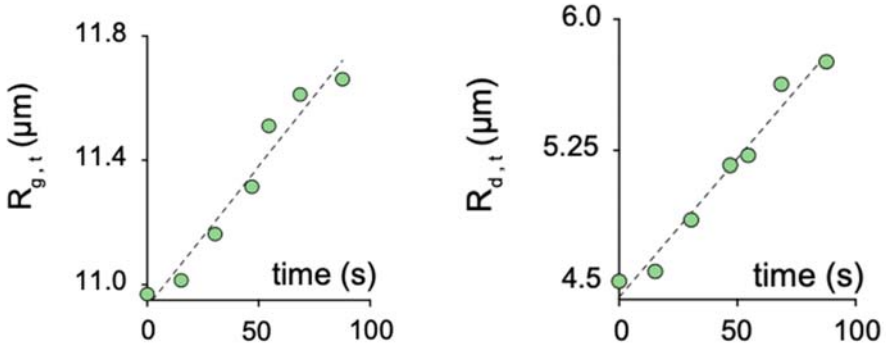

Figure 2: Plot of R_g and R_d as a function of time

S_t^{cap} can be calculated as follow:

$$S_t^{cap} = 2\pi {R_{g,t}}^2 . \left(1 - \sqrt{1 - (\frac{R_{d,t}}{R_{g,t}})^2}\right)$$

Following, we have S_t^{DEV}:

$$S_t^{DEV} = 2\pi {R_{g,t}}^2 . \left(1 + \sqrt{1 - (\frac{R_{d,t}}{R_{g,t}})^2}\right)$$

Compared to an equivalent droplet-free vesicle, the permeation area of the DEV must therefore be corrected by the following factor:

$$\beta_t = \frac{S_t^{DEV}}{S_t^{GUV}} = \frac{1}{2}\left(1 + \sqrt{1 - (\frac{R_{d,t}}{R_{g,t}})^2}\right)$$

Correction factor β_t:

As the radius of the vesicle ($R_{g,t}$) and the radius of the droplet ($R_{d,t}$) evolved during the osmotic swelling (**Figure 2**), we calculated β_t over time and found that it only varied from 0,922 to 0,899. These variations are represented in **Figure 3**.

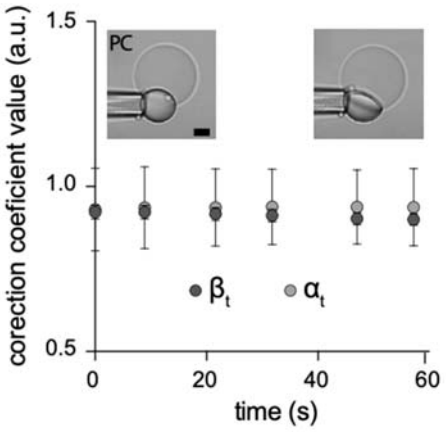

Figure 3: Plot of the correction coefficient α and β

In order to better quantify this small decrease of β_t , we calculated the ratio between the initial β_t and its value after 60 second of each osmotic swelling experiment (β_{60}/β_0, Figure 4, right). We find that β_t has very small variations: $2{,}15 \pm 0.67$ % and $1{,}04 \pm 0.69$ % respectively for To-DEV and Sq-DEV (**Figure 4, right**). Based on these observations, we considered $\beta_t = \beta_0$. We plotted all the value of β_0 in (**Figure 4, left**).

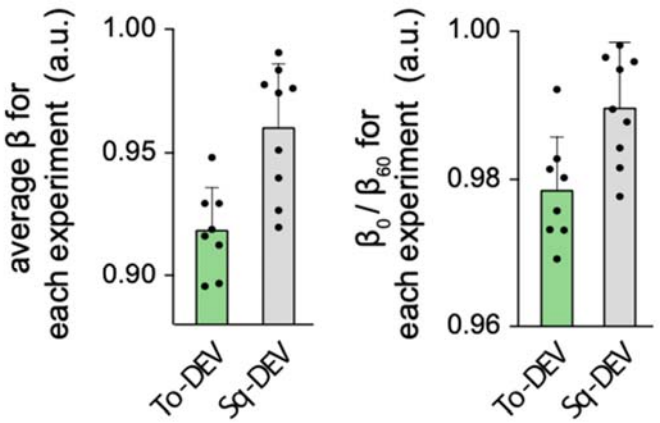

$$S_t^{DEV} = 4\pi R_{g,t}^2 . \beta_0$$

Figure 4: Left: Mean value of β for DEVs permeability assay; Right: Variations of β during permeability experiment.

We thus have a surface of permeation S_t which can written as:

$$S_t = \beta_0 . 4\pi {R_{g,t}}^2 \text{ for DEV and } S_t = 4\pi {R_{g,t}}^2 \text{ for GUVs}$$

D. GUV and DEV volume: hypothesis and computation as a function of $R_{g,t}$

For the volume of a GUV, V_t can be expressed as:

$$V_t^{GUV} = \frac{4}{3}\pi {R_{g,t}}^3$$

The inside DEV volume V_t^{DEV} has to be corrected because of the presence to the droplet:

$$V_t^{DEV} = V_t^{GUV} - V_t^{drop,in}$$

where $V_t^{drop,in}$ is the lacking of aqueous volume in the vesicle occupied by the embedded droplet (see Figure S1A). V_t^{DEV} can be expressed as:

$$V_t^{DEV} = \frac{4}{3}\pi {R_{g,t}}^3 - \frac{\pi}{3}(h_{out,t}^2(3R_{g,t} - h_{out,t}) + (h_{in,t}^2(3R_{drop,t}^{in} - h_{in,t})$$

where $h_{out,t}$, $h_{in,t}$ and $R_{drop,t}^{in}$ are all defined in **Figure 1**.

It follows:

$$\frac{V_t^{DEV}}{V_t^{GUV}} = 1 - \frac{(h_{out,t}^2(3R_{g,t} - h_{out,t}) + (h_{in,t}^2(3r_{drop,t}^{in} - h_{in}, t)}{4R_{g,t}^3} = \alpha_t$$

For the experiment in **figure 2** the variation of α_t are plotted as a function of time (**Figure 3**).

Correction factor α_t:

Where α_t is the correction factor of the DEV inner volume compared to the one of GUVs. As we did previously for β_t , α_t is plotted as a function of time (Figure 3). The variation of α_t is also very small, from 0,930 to 0,937. We also examined for each experiment the variations of α_t during the first 60 seconds α_{60}/α_0 (Figure 5, right) which were very small: $1{,}11 \pm 0.35$ % and $0{,}50 \pm 0.48$ % respectively for To-DEV and Sq-DEV (**Figure 5, right**). Based on these observations, we considered $\alpha_t = \alpha_0$. We plotted all the value of α_0 in (**Figure 5 left**).

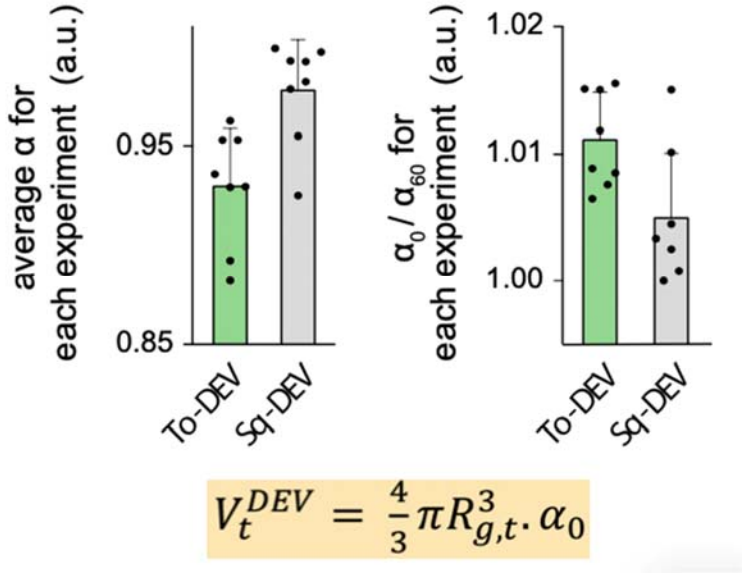

Figure 5: Left: Mean value of α for DEVs permeability assay; Right: Variations of α during permeability experiment.

In conclusion, the volume of permeation of a DEV and a GUV write as:

$$V_t = \alpha_0 . \frac{4}{3}\pi {R_{g,t}}^3 \quad \text{for DEVs and} \quad V_t = \frac{4}{3}\pi {R_{g,t}}^3 \quad \text{for GUVs}$$

E. Fick law with $R_{g,t}$ as the sole variable:

Considering the expression $\Delta C(t)$ established in B. one obtains:

$$\frac{dV_t}{dt} = -P . S_t . v_m . C_0^i . \left(\frac{C_0^e}{C_0^i} + 3\frac{R_{g,t}}{R_{g,0}} - 4 \right)$$

Replacing V_t *and* S_t by their expression obtained in C. and D leads to:

$$\frac{d(\alpha_0 . \frac{4}{3}\pi {R_{g,t}}^3)}{dt} = -P . \beta_0 . 4\pi {R_{g,t}}^2 . v_m . C_0^i . \left(\frac{C_0^e}{C_0^i} + 3\frac{R_{g,t}}{R_{g,0}} - 4 \right)$$

We obtain a differential equation of the first order with a constant second member:

$$\frac{d(\frac{R_{g,t}}{R_{g,0}})}{dt} + \frac{3P.\beta_0.\alpha_0^{-1}.v_m.C_0^i}{R_{g,0}}\frac{R_{g,t}}{R_{g,0}} = \frac{P.\beta_0.\alpha_0^{-1}.v_m.C_0^i}{R_{g,0}}.\left(4 - \frac{C_0^e}{C_0^i}\right)$$

So:

$$\frac{d\left(\frac{R_{g,t}}{R_{g,0}}\right)}{dt} + a\frac{R_{g,t}}{R_{g,0}} = \frac{a}{3}\left(4 - \frac{C_0^e}{C_0^i}\right) \quad \text{where} \quad a = \frac{3P.\beta_0.\alpha_0^{-1}.v_m.C_0^i}{R_{g,0}}$$

As we have linear curve for $\frac{R_{g,t}}{R_{g,0}}$ for the first 60 seconds (**Figure S1L**), $\frac{d\left(\frac{R_{g,t}}{R_{g,0}}\right)}{dt} = \omega$ is constant and equal to the slope of $\frac{R_{g,t}}{R_{g,0}}$.

$$\omega = (\left(4 - \frac{C_0^e}{C_0^i}\right) - 3\frac{< R_{g,t} >}{R_{g,0}})\frac{P_{initial}.\beta_0.\alpha_0^{-1}.v_m.C_0^i}{R_{g,0}}$$

Here, $P_{initial}$, "initial permeability" replaces the permeability because we considered only initial slope at the beginning of experiment. For a given experiment, $< R_{g,t} >$ is the mean of $R_{g,t}$ in the first 60 seconds.

$$P_{initial} = \frac{\omega.R_{g,0}}{\beta_0.\alpha_0^{-1}.v_m.((4-3\frac{<R_{g,t}>}{R_{g,0}})C_0^i - C_0^e)}$$

With this expression, we determined the initial permeability to water $P_{initial}$ for PC GUVs, PC triolein-DEVs and PC squalene-DEVs. (**Principal Figure 1E, left**)